

Theoretical support of experiments at high energy colliders

Renat Sadykov

DLNP JINR, Dubna, 26.09.2018

Outline

- **MCSANC** for Drell-Yan (DY) processes at hadron colliders
 - Motivation
 - Higher order electroweak (EW) corrections to DY
 - Tuned comparison between different codes for DY (NC and CC)
 - Conclusions and plans
- **ARIEl** – new project for precision study of e^+e^- collisions with polarized beams
 - Motivation and goals
 - Description of the project
 - Polarized Bhabha scattering $e^+e^- \rightarrow e^+e^-$ at **NLO EW**
 - Preliminary results at **NLO EW** for other processes with polarized e^+e^- beams
 - Conclusions and plans

Part I. MCSANC for Drell-Yan processes at hadron colliders

DY processes. Motivation

- The DY processes have leptonic final states with clean signatures
- Measurements are used for PDF constraints and SM verification
- Current fixed order precision is NNLO QCD + NLO EW (**FEWZ**, **DYNNLO**, **POWHEG**, **RADY**, **HORACE**, **MCSANC**)
- LHC gives access to energies where additional corrections have to be included:
 - photon-induced contributions
 - higher order radiative corrections
 - "missed" EW radiative corrections (IFI + ISR)

DY processes. Leading two-loop corrections

In **MCSANC v1.20** we follow the recipe introduced in [Phys.Lett. B319 (1993) 249-256].

The ρ parameter is defined as the ratio of the neutral current to charged current amplitudes at zero momentum transfer:

$$\rho = \frac{G_{NC}(0)}{G_{CC}(0)} = \frac{1}{1 - \Delta\rho},$$

where $G_{CC}(0) = G_\mu$ is the Fermi constant defined from the μ -decay width, perturbatively

$$\Delta\rho = \Delta\rho^{(1)} + \Delta\rho^{(2)} + \dots$$

We try to estimate the effect due to the two-loop EW corrections $\Delta\rho^{(2)}$ by basic replacements in our form factors (FF). Expanding ρ to quadratic terms $\Delta\rho^2$, we have

$$\rho = 1 + \Delta\rho + \Delta\rho^2.$$

DY processes. Leading two-loop corrections

The leading in $G_\mu m_t^2$ NLO EW contribution to $\Delta\rho$ is explicitly given by

$$\Delta\rho^{(1)}\Big|^{G_\mu} = 3x_t = \frac{3\sqrt{2}G_\mu m_t^2}{16\pi^2}.$$

At the two-loop level, quantity $\Delta\rho$ contains two contributions:

$$\Delta\rho = 3x_t \left[1 + \rho^{(2)} \left(M_H^2/m_t^2 \right) x_t \right] \left[1 - \frac{2\alpha_s(M_Z^2)}{9\pi} (\pi^2 + 3) \right].$$

They consist of the following:

- two-loop EW part at $\mathcal{O}(G_\mu^2)$.
- mixed two-loop EW \otimes QCD at $\mathcal{O}(G_\mu\alpha_s)$

DY processes. Leading two-loop corrections

Using intermediate vector boson propagators $\sim 1/(Q^2 + M_V^2)$, we derive:

$$\rho = \frac{M_W^2}{\bar{c}_W^2 M_Z^2},$$

where we introduced a new parameter \bar{c}_W^2 to distinguish from the usual c_W^2 for which we maintain the meaning $c_W^2 = M_W^2/M_Z^2$ to be valid to all perturbative orders. At the lowest order (LO)

$$\rho^{(0)} = \frac{M_W^2}{c_W^2 M_Z^2} = 1.$$

Then:

$$\bar{c}_W^2 = \frac{M_W^2}{\rho M_Z^2} = (1 - \Delta\rho) c_W^2.$$

DY processes. Leading two-loop corrections

The leading in $G_\mu m_t^2$ universal higher order (h.o.) corrections may be taken into account. via the replacements, [JHEP 1001 (2010) 060]:

$$\begin{aligned}\alpha_{G_\mu} &\rightarrow \alpha_{G_\mu} \frac{\bar{s}_W^2}{s_W^2}, \\ s_W^2 &\rightarrow \bar{s}_W^2 \equiv s_W^2 + \Delta\rho c_W^2, \\ c_W^2 &\rightarrow \bar{c}_W^2 \equiv 1 - \bar{s}_W^2 = (1 - \Delta\rho) c_W^2\end{aligned}$$

in the LO expression for NC DY cross section.

This approach correctly reproduces terms up to $\mathcal{O}(\Delta\rho^2)$.

Given these replacements, we get the contributions of h.o. corrections to the scalar form factors of the invariant amplitude

DY processes. Leading two-loop corrections

In the LQ basis the Z exchange amplitude has the following Born-like structure in terms of four (LL , QL , LQ and QQ) form factors:

$$\mathcal{A}_Z^{\text{IBA}} = -i \frac{4\pi\alpha}{s} \left[\frac{1}{4s_W^2 c_W^2} \frac{s}{s - M_Z^2 + i \frac{\Gamma_Z}{M_Z} s} \right]$$

$$\cdot \left\{ \begin{aligned} & \gamma_\mu \gamma_+ \otimes \gamma_\mu \gamma_+ I_e^{(3)} I_t^{(3)} F_{LL}(s, t), \\ & + \gamma_\mu \otimes \gamma_\mu \gamma_+ (-2Q_e s_W^2) I_t^{(3)} F_{QL}(s, t) \\ & + \gamma_\mu \gamma_+ \otimes \gamma_\mu I_e^{(3)} (-2Q_f s_W^2) F_{LQ}(s, t) \\ & + \gamma_\mu \otimes \gamma_\mu (-2Q_e s_W^2) (-2Q_f s_W^2) F_{QQ}(s, t) \end{aligned} \right\},$$

DY processes. Leading two-loop corrections

$$\begin{aligned}
 \mathcal{A}_Z^{\text{IBA}}(\text{with h.o.}) = & i \frac{4\pi\bar{\alpha}G_\mu}{s} \left[\frac{1}{4} \frac{1}{s_W^2} \begin{bmatrix} s_W^2 \\ -s_W^2 \end{bmatrix} \frac{s}{s - M_Z^2 + i \frac{\Gamma_Z}{M_Z} s} \right] \\
 & \left\{ \gamma_\mu \gamma_+ \otimes \gamma_\mu \gamma_+ I_e^{(3)} I_t^{(3)} \begin{bmatrix} 1 \\ -e_W^2 \end{bmatrix} F_{LL}(s, t), \right. \\
 & + \gamma_\mu \otimes \gamma_\mu \gamma_+ (-2Q_e) s_W^2 \begin{bmatrix} s_W^2 & 1 \\ s_W^2 & -e_W^2 \end{bmatrix} I_t^{(3)} F_{QL}(s, t) \\
 & + \gamma_\mu \gamma_+ \otimes \gamma_\mu I_e^{(3)} (-2Q_f) s_W^2 \begin{bmatrix} s_W^2 & 1 \\ s_W^2 & -e_W^2 \end{bmatrix} F_{LQ}(s, t) \\
 & \left. + \gamma_\mu \otimes \gamma_\mu (-2Q_e) (-2Q_f) s_W^4 \begin{bmatrix} s_W^4 & 1 \\ s_W^4 & -e_W^2 \end{bmatrix} F_{QQ}(s, t) \right\},
 \end{aligned}$$

where for convenience, we multiply and divide s_W^2 on the expression s_W^2/s_W^2

DY processes. Leading two-loop corrections

The object $\frac{1}{e_w^2}$ will go into:

$$\frac{1}{e_w^2} = \frac{1}{(1 - \Delta\rho)c_w^2} = (1 + \Delta\rho + \Delta\rho^2) \frac{1}{c_w^2},$$

and the object $\frac{s_w^2}{s_w^2}$ will go into:

$$\frac{s_w^2}{s_w^2} = (1 + \frac{c_w^2}{s_w^2} \Delta\rho).$$

DY processes. Leading two-loop corrections

Therefore, amplitude in NNLO order is:

$$\begin{aligned}
 \mathcal{A}_Z^{\text{IBA}}(\text{with } h.o.) = & \\
 & \cdot -i \frac{4\pi\alpha_{G_\mu}}{s} \left[\frac{1}{4s_W^2 c_W^2} \frac{s}{s - M_Z^2 + i \frac{\Gamma_Z}{M_Z} s} \right] \\
 & \left\{ \gamma_\mu \gamma_+ \otimes \gamma_\mu \gamma_+ I_e^{(3)} I_t^{(3)} [1 + \Delta\rho + \Delta\rho^2] F_{LL}(s, t) \right. \\
 & + \gamma_\mu \otimes \gamma_\mu \gamma_+ (-2Q_e) s_W^2 \left[(1 + \Delta\rho + \Delta\rho^2) \left(1 + \frac{c_W^2}{s_W^2} \Delta\rho\right) \right] I_t^{(3)} F_{QL}(s, t) \\
 & + \gamma_\mu \gamma_+ \otimes \gamma_\mu I_e^{(3)} (-2Q_f) s_W^2 \left[(1 + \Delta\rho + \Delta\rho^2) \left(1 + \frac{c_W^2}{s_W^2} \Delta\rho\right) \right] F_{LQ}(s, t) \\
 & \left. + \gamma_\mu \otimes \gamma_\mu (-2Q_e) (-2Q_f) s_W^4 \left[(1 + \Delta\rho + \Delta\rho^2) \left(1 + \frac{c_W^2}{s_W^2} \Delta\rho\right)^2 \right] F_{QQ}(s, t) \right\},
 \end{aligned}$$

DY processes. Leading two-loop corrections

To avoid a double counting one should remove the leading NLO EW contribution from the linear in $\Delta\rho$ terms: $\Delta\rho \longrightarrow \left(\Delta\rho - \Delta\rho^{(1)} \Big|^{G_\mu} \right)$.

We showed analytically that the results obtained in this way agree with the corresponding expressions from paper [JHEP 1001 (2010) 060].

A large group of dominant radiative corrections can be absorbed into the shift of the ρ parameter from its lowest order value $\rho_{Born} = 1$.

These groups of radiative corrections are:

$$\begin{aligned} \Delta\rho = & \Delta\rho_{x_t} + \Delta\rho_{\alpha\alpha_s} + \Delta\rho_{x_t\alpha_s^2} + \left(\Delta\rho_{x_t(zt)\alpha_s^2} + \Delta\rho_{x_t(alp)_f^2} \right) \\ & + \Delta\rho_{x_t\alpha_s^3} + \Delta\rho_{x_t^2\alpha_s} + \Delta\rho_{x_t^2(bos)} + \Delta\rho_{x_t^3}. \end{aligned}$$

DY processes. Leading two-loop corrections

Instead of complete calculation of all perturbative orders, the dominant radiative corrections can be absorbed into the shift of the ρ parameter from it's lowest order value $\rho_{Born} = 1$:

$$\begin{aligned}\Delta\rho = & \Delta\rho_{x_t} + \Delta\rho_{\alpha\alpha_s} + \Delta\rho_{x_t\alpha_s^2} + \left(\Delta\rho_{x_t(zt)\alpha_s^2} + \Delta\rho_{x_t(alp)_f^2} \right) \\ & + \Delta\rho_{x_t\alpha_s^3} + \Delta\rho_{x_t^2\alpha_s} + \Delta\rho_{x_t^2(bos)} + \Delta\rho_{x_t^3}\end{aligned}$$

For simplicity denote the corrections with indices:

notation	order of	DIZET v6.42	MCSANC
$\Delta\rho_1$	$O(\alpha\alpha_s)$	+	+
$\Delta\rho_2$	$O(\alpha^2)$	+	+
$\Delta\rho_3$	$O(\alpha_t\alpha_s^2)$	+	+
$\Delta\rho_4$	$O(\alpha_t^2\alpha_s)$	-	+
$\Delta\rho_5$	$O(\alpha_t\alpha_s^3)$	-	+

DY processes. Tuned comparison

- We participated in tuned comparison of different codes for Drell-Yan processes at hadron colliders in the context of *LPCC Electroweak Precision Measurements at the LHC WG*. The results were published in *Eur.Phys.J. C77 (2017) no.5, 280*. The relevant codes can be found at: <https://twiki.cern.ch/twiki/bin/view/Main/DrellYanComparison>
- Now we invited to participate in new comparison within *W-mass 2018 worksop*. For this comparison we will use our MC generator.

DY processes. Tuned comparison. Setup

Input parameters:

$$\sqrt{s} = 8 \text{ GeV},$$

$$G_\mu = 1.1663787 \times 10^{-5} \text{ GeV}^{-2},$$

$$M_Z = 91.1876 \text{ GeV},$$

$$M_W = 80.385 \text{ GeV},$$

$$M_H = 125 \text{ GeV},$$

$$m_e = 0.510998928 \text{ MeV},$$

$$m_u = 0.06983 \text{ GeV},$$

$$m_d = 0.06984 \text{ GeV},$$

$$|V_{ud}| = 0.975,$$

$$|V_{cd}| = 0.222,$$

$$|V_{cb}| = |V_{ts}| = |V_{ub}| = |V_{td}| = |V_{tb}| = 0.$$

$$\alpha = 1/137.035999074, \quad \alpha_s \equiv \alpha_s(M_Z^2) = 0.12018,$$

$$\Gamma_Z = 2.4952 \text{ GeV},$$

$$\Gamma_W = 2.085 \text{ GeV},$$

$$m_\mu = 0.1056583715 \text{ GeV}, \quad m_\tau = 1.77682 \text{ GeV},$$

$$m_c = 1.2 \text{ GeV}, \quad m_t = 173.5 \text{ GeV},$$

$$m_s = 0.15 \text{ GeV}, \quad m_b = 4.6 \text{ GeV},$$

$$|V_{us}| = 0.222,$$

$$|V_{cs}| = 0.975,$$

DY processes. Tuned comparison. Setup

The detector acceptance is simulated by imposing the following transverse momentum (p_{\perp}) and pseudo-rapidity (η) cuts:

$$\text{LHC:} \quad p_{\perp}^{\ell} > 25 \text{ GeV}, \quad |\eta(\ell)| < 2.5, \quad p_{\perp}^{\nu} > 25 \text{ GeV}, \quad \ell = e, \mu,$$

where p_{\perp}^{ν} is the missing transverse momentum originating from the neutrino. These cuts approximately model the acceptance of the ATLAS and CMS detectors at the LHC. In addition we apply a cut on the invariant mass of the final-state lepton pair of $M_{l+l-} > 50 \text{ GeV}$ and $M(l\nu) > 1 \text{ GeV}$ in the case of γ/Z production and W production respectively.

DY processes. Tuned comparison for W^+ production

code	LO	NLO QCD	NLO EW μ	NLO EW e
HORACE	2897.38(8)	×	2988.2(1)	2915.3(1)
WZGRAD	2897.33(2)	×	2987.94(5)	2915.39(6)
RADY	2897.35(2)	2899.2(4)	2988.01(4)	2915.38(3)
SANC	2897.30(2)	2899.9(3)	2987.77(3)	2915.00(3)
DYNNLO	2897.32(5)	2899(1)	×	×
FEWZ	2897.2(1)	2899.4(3)	×	×
POWHEG-w	2897.34(4)	2899.41(9)	×	×
POWHEG_BMNNP	2897.36(5)	2899.0(1)	2988.4(2)	2915.7(1)
POWHEG_BW	2897.4(1)	2899.2(3)	2987.7(4)	(×)

DY processes. Tuned comparison for W^- production

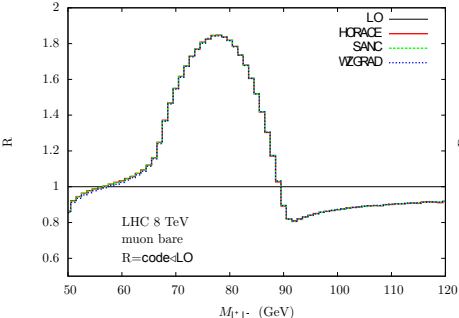
code	LO	NLO QCD	NLO EW μ	NLO EW e
HORACE	2008.84(5)	×	2076.48(9)	2029.15(8)
WZGRAD	2008.95(1)	×	2076.51(3)	2029.26(3)
RADY	2008.93(1)	2050.5(2)	2076.62(2)	2029.29(2)
SANC	2008.926(8)	2050.3(3)	2076.56(2)	2029.19(3)
DYNNLO	2008.89(3)	2050.2(9)	×	×
FEWZ	2008.9(1)	2049.97(8)	×	×
POWHEG-w	2008.93(3)	2050.14(5)	×	×
POWHEG_BMNNP	2008.94(3)	2049.9(1)	2076.9(1)	2029.71(6)
POWHEG_BW	2009.2(4)	2050.2(4)	2076.0(3)	(×)

DY processes. Tuned comparison for Z production

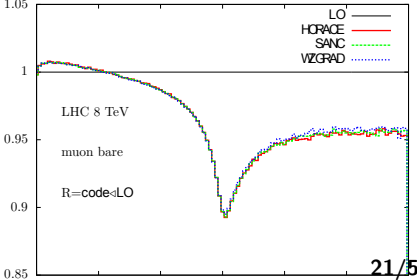
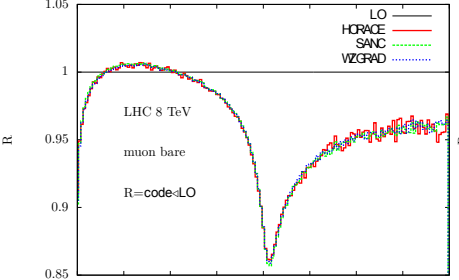
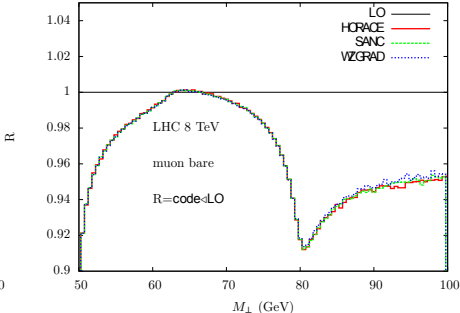
code	LO	NLO QCD	NLO EW μ	NLO EW e
HORACE	431.033(9)	×	438.74(2)	422.08(2)
WZGRAD	431.048(7)	×	439.166(6)	422.78(1)
RADY	431.047(4)	458.16(3)	438.963(4)	422.536(5)
SANC	431.050(2)	458.27(3)	439.004(5)	422.56(1)
DYNNLO	431.043(8)	458.2(2)	×	×
FEWZ	431.00(1)	458.13(2)	(×)	(×)
POWHEG-z	431.08(4)	458.19(8)	×	×
POWHEG_BMNNPV	431.046(9)	458.16(7)	438.9(1)	422.2(2)

DY processes. Tuned comparison

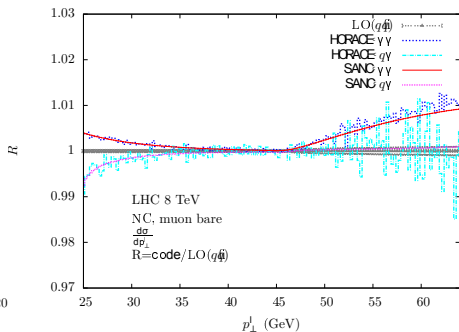
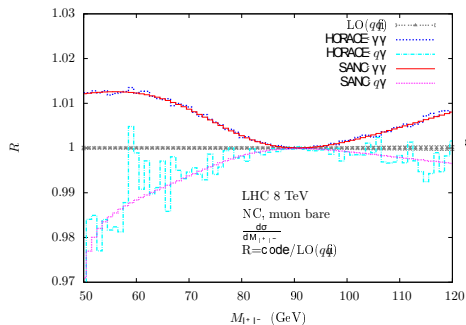
Z-production



W^+ -production



DY processes. Tuned comparison for photon induced contributions

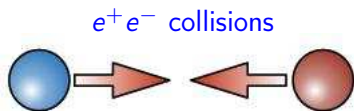


Conclusions and plans

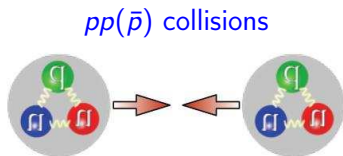
- We participated in tuned comparison of different codes for DY processes at LHC
- New tuned comparison 2018-2019
- A set of HO leading corrections are introduced to the MCSANC generator
- Working on new tool **DYTURBO**: SANC EW library

Part II. ARLeL - new project for future e^+e^- colliders

Motivation: choice of collider types



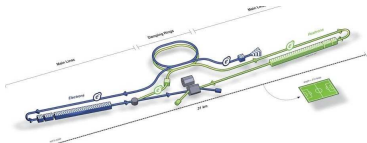
- Point-like particles
- Total annihilation: initial state known
- Decent background
- Limited in energy, but — **precision!**



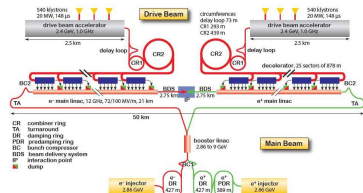
- Composite particles
- Random energy of the hard interaction
- High background
- High energy — **discovery!**

Projects of e^+e^- collider

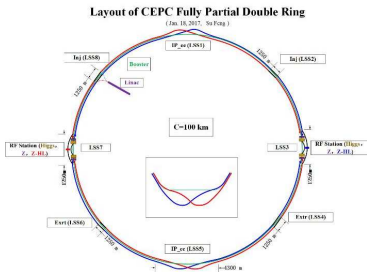
ILC (2030) 250 GeV



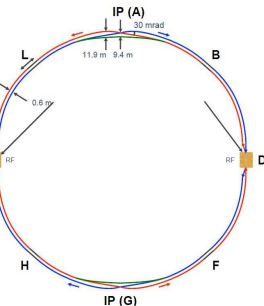
CLIC (2035) 380-3000 GeV



CEPC (2030) 240 GeV



FCC-ee (2039) 350 GeV



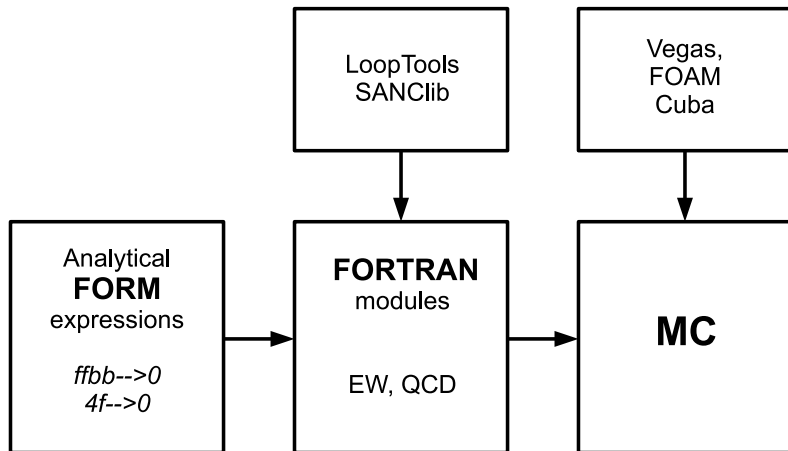
Why ARIeL?

- **A**dvanced
- **R**esearch of
- **I**nteractions in
- e^+e^-
- **coL**lisions

Goals

- Preparation of CLIC research program:
 - Precision study of $e^+e^- \rightarrow \gamma\gamma$ and setting limits on the NP models
 - Precision measurement of the Higgs boson mass M_H
 - Determination of top quark polarization
 - Measurement of $\gamma\gamma \rightarrow W^+W^-$ and $\gamma\gamma \rightarrow ZZ$ and search for anomalous quaring coupling
- Theoretical support:
 - Create e^+e^- Monte Carlo generator with polarization at **complete one-loop EW** and **leading multiloop** for processes $e^+e^- \rightarrow e^+e^- (\mu\mu, \tau\tau, tt, HZ, H\gamma, Z\gamma, ZZ, H\nu\nu, H\mu\mu, f\bar{f}\gamma, \gamma\gamma)$
 - Interface NLO EW RC to PYTHIA8
 - Implement a single-resonance approach to complex processes
 - Elaborate the standard procedure for $2 \rightarrow 3, 4$ helicity amplitudes
 - Create building blocks for complete EW 2-loops and QCD 3-loops, plus leading EW 3-loops and QCD 4-loops

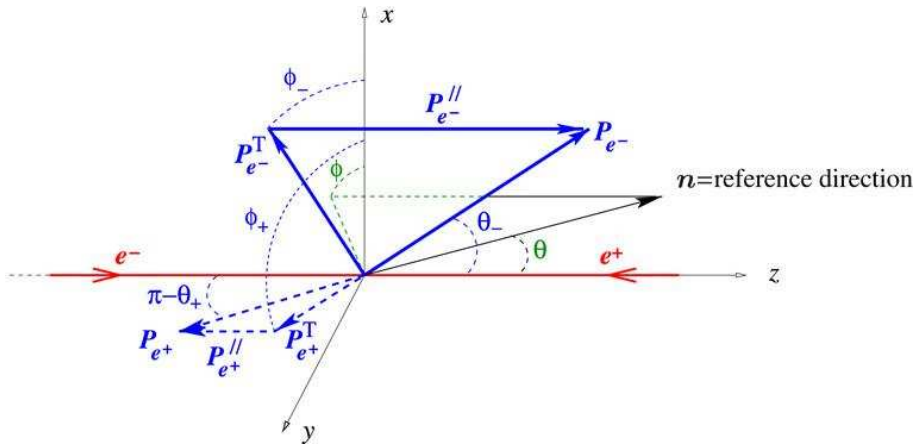
The calculation framework scheme



Processes with polarized beams in MCSAN Cee

- NLO EW corrections for polarized e^+e^- scattering:
 - Bhabha scattering (D.Bardin et al. Phys.Rev. D98 (2018) no.1, 013001)
 - $e^+e^- \rightarrow \mu^+\mu^-$, $e^+e^- \rightarrow \tau^+\tau^-$ (preliminary results)
 - $e^+e^- \rightarrow Z\gamma$ (preliminary results)
 - $e^+e^- \rightarrow t\bar{t}$ (in progress)
 - $e^+e^- \rightarrow ZH$ (in progress)
 - $e^+e^- \rightarrow \gamma\gamma$ (in progress)
 - $e^+e^- \rightarrow ZZ$ (in progress)
 - $e^+e^- \rightarrow f\bar{f}\gamma$ (future plans)
 - $e^+e^- \rightarrow f\bar{f}H$ (future plans)
- NLO EW corrections for polarized $\gamma\gamma$ scattering:
 - $\gamma\gamma \rightarrow \gamma\gamma$ (future plans)
 - $\gamma\gamma \rightarrow Z\gamma$ (future plans)
 - $\gamma\gamma \rightarrow ZZ$ (future plans)

Decomposition of the e^\pm polarization vector



G. Moortgat-Pick et al. Phys. Rept. 460 (2008) 131–243

Matrix element squared

$$\begin{aligned}
 |\mathcal{M}|^2 = & L_{e^-}^{\parallel} R_{e^+}^{\parallel} |\mathcal{H}_{-+}|^2 + R_{e^-}^{\parallel} L_{e^+}^{\parallel} |\mathcal{H}_{+-}|^2 + L_{e^-}^{\parallel} L_{e^+}^{\parallel} |\mathcal{H}_{--}|^2 + R_{e^-}^{\parallel} R_{e^+}^{\parallel} |\mathcal{H}_{++}|^2 \\
 & - \frac{1}{2} P_{e^-}^T P_{e^+}^T \operatorname{Re} \left[e^{i(\Phi_+ - \Phi_-)} \mathcal{H}_{++} \mathcal{H}_{--}^* + e^{i(\Phi_+ + \Phi_-)} \mathcal{H}_{+-} \mathcal{H}_{-+}^* \right] \\
 & + P_{e^-}^T \operatorname{Re} \left[e^{i\Phi_-} \left(L_{e^+}^{\parallel} \mathcal{H}_{+-} \mathcal{H}_{--}^* + R_{e^+}^{\parallel} \mathcal{H}_{++} \mathcal{H}_{-+}^* \right) \right] \\
 & - P_{e^+}^T \operatorname{Re} \left[e^{i\Phi_+} \left(L_{e^-}^{\parallel} \mathcal{H}_{-+} \mathcal{H}_{--}^* + R_{e^-}^{\parallel} \mathcal{H}_{++} \mathcal{H}_{+-}^* \right) \right],
 \end{aligned}$$

where

$$L_{e^\pm}^{\parallel} = \frac{1}{2}(1 - P_{e^\pm}^{\parallel}), \quad R_{e^\pm}^{\parallel} = \frac{1}{2}(1 + P_{e^\pm}^{\parallel}), \quad \Phi_{\pm} = \phi_{\pm} - \phi,$$

$\mathcal{H}_{--}, \mathcal{H}_{++}, \mathcal{H}_{-+}, \mathcal{H}_{+-}$ — helicity amplitudes.

Longitudinally-polarized beams

With longitudinally-polarized beams, cross-sections at an e^+e^- collider can be subdivided into four parts:

$$\sigma_{P_{e^-}P_{e^+}} = R_{e^-}R_{e^+}\sigma_{RR} + L_{e^-}L_{e^+}\sigma_{LL} + R_{e^-}L_{e^+}\sigma_{RL} + L_{e^-}R_{e^+}\sigma_{LR},$$

where σ_{RL} stands for the cross-section if the e^- beam is completely right-handed polarized ($P_{e^-} = +1$) and the e^+ beam is completely left-handed polarized ($P_{e^+} = -1$). The cross-sections σ_{LR} , σ_{RR} and σ_{LL} are defined analogously.

Polarized Bhabha scattering at one-loop

Here we present complete one-loop EW corrections to Bhabha scattering $e^+e^- \rightarrow e^+e^-$ with longitudinally polarized initial particles.

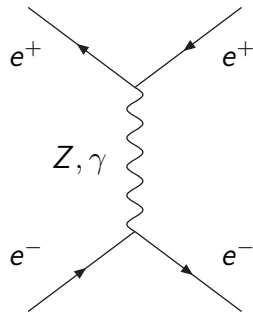
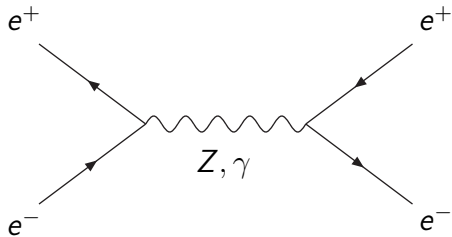
The cross-section of this process at one-loop can be divided into four parts:

$$\sigma^{1\text{-loop}} = \sigma^{\text{Born}} + \sigma^{\text{virt}}(\lambda) + \sigma^{\text{soft}}(\lambda, \omega) + \sigma^{\text{hard}}(\omega),$$

where σ^{Born} — Born level cross-section, σ^{virt} — contribution of virtual(loop) corrections, σ^{soft} — contribution due to soft photon emission, σ^{hard} — contribution due to hard photon emission (with energy $E_\gamma > \omega \frac{\sqrt{s}}{2}$).

Auxiliary parameters λ ("photon mass") and ω cancel out after summation.

Bhabha scattering: Born-level diagrams



Polarized Bhabha scattering: HA for Born and Virtual parts

At one-loop level we have six non-zero HAs (four independent):

$$\begin{aligned}
 \mathcal{H}_{++++} &= \mathcal{H}_{----} = -2e^2 \frac{s}{t} \left(\mathcal{F}_{QQ}^{(\gamma, Z)}(t, s, u) - \chi_Z^t \delta_e \mathcal{F}_{QL}^Z(t, s, u) \right), \\
 \mathcal{H}_{+--+} &= \mathcal{H}_{-+-+} = -2e^2 \frac{t}{s} \left(\mathcal{F}_{QQ}^{(\gamma, Z)}(s, t, u) - \chi_Z^s \delta_e \mathcal{F}_{QL}^Z(s, t, u) \right), \\
 \mathcal{H}_{+---} &= 2e^2 \left(\frac{u}{s} \left[\mathcal{F}_{QQ}^{(\gamma, Z)}(s, t, u) + \chi_Z^s (\mathcal{F}_{LL}^Z(s, t, u) - 2\delta_e \mathcal{F}_{QL}^Z(s, t, u)) \right] \right. \\
 &\quad \left. + \frac{u}{t} \left[\mathcal{F}_{QQ}^{(\gamma, Z)}(t, s, u) + \chi_Z^t (\mathcal{F}_{LL}^Z(t, s, u) - 2\delta_e \mathcal{F}_{QL}^Z(t, s, u)) \right] \right), \\
 \mathcal{H}_{-++-} &= 2e^2 \left(\frac{u}{s} \mathcal{F}_{QQ}^{(\gamma, Z)}(s, t, u) + \frac{u}{t} \mathcal{F}_{QQ}^{(\gamma, Z)}(t, s, u) \right),
 \end{aligned}$$

where

$$\chi_Z^s = \frac{1}{4s_W^2 c_W^2} \frac{s}{s - M_Z^2 + iM_Z \Gamma_Z}, \quad \chi_Z^t = \frac{1}{4s_W^2 c_W^2} \frac{t}{t - M_Z^2}, \quad \delta_e = v_e - a_e = 2s_W^2,$$

$$\mathcal{F}_{QQ}^{(\gamma, Z)}(a, b, c) = \mathcal{F}_{QQ}^\gamma(a, b, c) + \chi_Z^a \delta_e^2 \mathcal{F}_{QQ}^Z(a, b, c).$$

We get the Born level HAs by replacing $\mathcal{F}_{LL}^Z \rightarrow 1$, $\mathcal{F}_{QL}^Z \rightarrow 1$, $\mathcal{F}_{QQ}^Z \rightarrow 1$ and $\mathcal{F}_{QQ}^\gamma \rightarrow 1$.

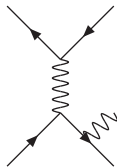
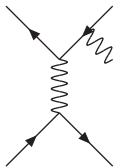
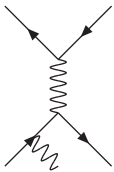
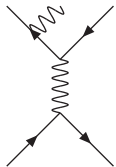
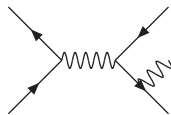
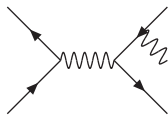
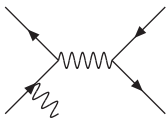
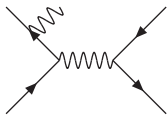
Polarized Bhabha scattering: soft photon contribution

The soft photon contribution contains the infrared divergences which compensate the infrared divergences of the one-loop QED corrections.

This soft photon correction can be calculated analytically and to be factorized to Born cross section. The polarization dependence is contained in σ^{Born} .

$$\begin{aligned}\sigma^{\text{soft}}(\lambda, \omega) &= -\sigma^{\text{Born}} \frac{\alpha}{\pi} \left\{ \left(1 + \ln \left(\frac{m_e^2}{s} \right) \right)^2 + \ln \left(-\frac{u}{s} \right)^2 - \ln \left(-\frac{t}{s} \right)^2 \right. \\ &\quad - 2\text{Li}_2 \left(-\frac{u}{s} \right) + 2\text{Li}_2 \left(-\frac{t}{s} \right) + 4\text{Li}_2(1) \\ &\quad \left. - 1 + 2 \ln \left(\frac{4\omega^2}{\lambda} \right) \left[1 + \ln \left(\frac{m_e^2}{s} \right) - \ln \left(\frac{t}{u} \right) \right] \right\}.\end{aligned}$$

Polarized Bhabha scattering: hard photon contribution



Polarized Bhabha scattering: hard photon contribution

Bremsstrahlung Helicity Amplitudes:

$$\mathcal{H}^{\text{hard}} = \mathcal{H}^{\text{isr}} + \mathcal{H}^{\text{fsr}}$$

Crossing symmetry:

$$\mathcal{H}_{\chi_1\chi_2\chi_3\chi_4\chi_5}^{\text{fsr}}(p_1, p_2, p_3, p_4) = +\mathcal{H}_{-\chi_4-\chi_3-\chi_2-\chi_1\chi_5}^{\text{isr}}(-p_4, -p_3, -p_2, -p_1)$$

CP-symmetry:

$$\mathcal{H}_{\chi_1\chi_2\chi_3\chi_4\chi_5}^{\text{hard}} = -\chi_1\chi_2\chi_3\chi_4\overline{\mathcal{H}}_{-\chi_1-\chi_2-\chi_3-\chi_4-\chi_5}^{\text{hard}}$$

Polarized Bhabha scattering: Monte Carlo generator

We created Monte Carlo generator of unweighted events for the polarized Bhabha scattering $e^+e^- \rightarrow e^+e^-$ with complete one-loop EW corrections.

This generator uses adaptive algorithm **mFOAM** [CPC 177:441-458,2007] which is a part of **ROOT** [<https://root.cern.ch>] program.

It will be interfaced to **PYTHIA8** [CPC 178 (2008) 852–867] program.

Setup for tuned comparison

We performed a tuned comparison of our results for polarized Born and hard Bremsstrahlung with the results **WHIZARD** [Eur.Phys.J.C71 (2011) 1742] program. The contributions of soft and virtual parts were compared with the results of **a1TALC** [CPC 174 (2006) 71-82] program

Input parameters:

$$\alpha^{-1}(0) = 137.03599976,$$

$$M_W = 80.4514958 \text{ GeV}, \quad M_Z = 91.1876 \text{ GeV}, \quad \Gamma_Z = 2.49977 \text{ GeV},$$

$$m_e = 0.51099907 \text{ MeV}, \quad m_\mu = 0.105658389 \text{ GeV}, \quad m_\tau = 1.77705 \text{ GeV},$$

$$m_d = 0.083 \text{ GeV}, \quad m_s = 0.215 \text{ GeV}, \quad m_b = 4.7 \text{ GeV},$$

$$m_u = 0.062 \text{ GeV}, \quad m_c = 1.5 \text{ GeV}, \quad m_t = 173.8 \text{ GeV}.$$

Cuts:

$$|\cos\theta| < 0.9,$$

$$E_\gamma > 1 \text{ GeV} \quad (\text{for comparison of hard Bremsstrahlung}).$$

$e^+e^- \rightarrow e^+e^-$: **WHIZARD** vs **MCSAN**Cee (Born)

P_{e^-}, P_{e^+}	0, 0	-0.8, 0	-0.8, -0.6	-0.8, 0.6
$\sqrt{s} = 250 \text{ GeV}$				
$\sigma_{e^+e^-}^{\text{Born}}$, pb	56.677(1)	57.774(1)	56.272(1)	59.276(1)
$\sigma_{e^+e^-}^{\text{Born}}$, pb	56.677(1)	57.775(1)	56.272(1)	59.275(1)
$\sqrt{s} = 500 \text{ GeV}$				
$\sigma_{e^+e^-}^{\text{Born}}$, pb	14.379(1)	15.030(1)	12.706(1)	17.355(1)
$\sigma_{e^+e^-}^{\text{Born}}$, pb	14.379(1)	15.030(1)	12.706(1)	17.354(1)
$\sqrt{s} = 1000 \text{ GeV}$				
$\sigma_{e^+e^-}^{\text{Born}}$, pb	3.6792(1)	3.9057(1)	3.0358(1)	4.7756(1)
$\sigma_{e^+e^-}^{\text{Born}}$, pb	3.6792(1)	3.9057(1)	3.0358(1)	4.7755(1)

$e^+e^- \rightarrow e^+e^-$: **WHIZARD** vs **MCSAN**Cee (hard)

P_{e^-}, P_{e^+}	0, 0	-0.8, 0	-0.8, -0.6	-0.8, 0.6
$\sqrt{s} = 250$ GeV				
$\sigma_{e^+e^-}^{\text{hard}}$, pb	48.62(1)	49.58(1)	48.74(1)	50.40(1)
$\sigma_{e^+e^-}^{\text{hard}}$, pb	48.65(1)	49.56(1)	48.78(1)	50.44(1)
$\sqrt{s} = 500$ GeV				
$\sigma_{e^+e^-}^{\text{hard}}$, pb	15.14(1)	15.81(1)	13.54(1)	18.07(1)
$\sigma_{e^+e^-}^{\text{hard}}$, pb	15.12(1)	15.79(1)	13.55(1)	18.11(2)
$\sqrt{s} = 1000$ GeV				
$\sigma_{e^+e^-}^{\text{hard}}$, pb	4.693(1)	4.976(1)	3.912(1)	6.041(1)
$\sigma_{e^+e^-}^{\text{hard}}$, pb	4.694(1)	4.975(1)	3.913(1)	6.043(1)

$e^+e^- \rightarrow e^+e^-$: **aĠTALC** vs **MCSAN**Cee
 (virtual+soft)

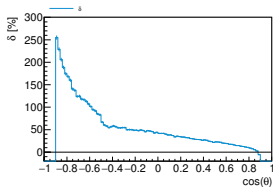
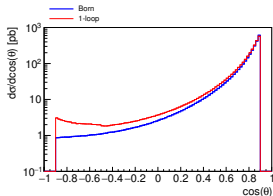
$\cos \theta$	$\sigma_{e^+e^-}^{\text{Born}}$, pb	$\sigma_{e^+e^-}^{\text{Born+virt+soft}}$, pb
-0.9	2.16999 $\cdot 10^{-1}$ 2.16999 $\cdot 10^{-1}$	1.93445 $\cdot 10^{-1}$ 1.93445 $\cdot 10^{-1}$
-0.5	2.61360 $\cdot 10^{-1}$ 2.61360 $\cdot 10^{-1}$	2.38707 $\cdot 10^{-1}$ 2.38707 $\cdot 10^{-1}$
0	5.98142 $\cdot 10^{-1}$ 5.98142 $\cdot 10^{-1}$	5.46677 $\cdot 10^{-1}$ 5.46677 $\cdot 10^{-1}$
+0.5	4.21273 $\cdot 10^0$ 4.21273 $\cdot 10^0$	3.81301 $\cdot 10^0$ 3.81301 $\cdot 10^0$
+0.9	1.89160 $\cdot 10^2$ 1.89160 $\cdot 10^2$	1.72928 $\cdot 10^2$ 1.72928 $\cdot 10^2$
+0.99	2.06556 $\cdot 10^4$ 2.06555 $\cdot 10^4$	1.90607 $\cdot 10^4$ 1.90607 $\cdot 10^4$
+0.999	2.08236 $\cdot 10^6$ 2.08236 $\cdot 10^6$	1.91624 $\cdot 10^6$ 1.91624 $\cdot 10^6$
+0.9999	2.08429 $\cdot 10^8$ 2.08429 $\cdot 10^8$	1.91402 $\cdot 10^8$ 1.91402 $\cdot 10^8$

$e^+e^- \rightarrow e^+e^-$: Born vs 1-loop

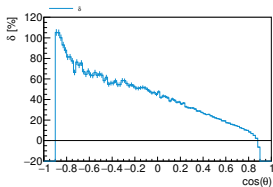
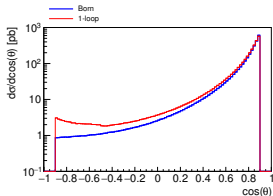
P_{e^-}, P_{e^+}	0, 0	-0.8, 0	-0.8, -0.6	-0.8, 0.6
$\sqrt{s} = 250 \text{ GeV}$				
$\sigma_{e^+e^-}^{\text{Born}}$, pb	56.6763(1)	57.7738(1)	56.2725(4)	59.2753(5)
$\sigma_{e^+e^-}^{\text{1-loop}}$, pb	61.731(6)	62.587(6)	61.878(6)	63.287(7)
δ , %	8.92(1)	8.33(1)	9.96(1)	6.77(1)
$\sqrt{s} = 500 \text{ GeV}$				
$\sigma_{e^+e^-}^{\text{Born}}$, pb	14.3789(1)	15.0305(1)	12.7061(1)	17.3550(2)
$\sigma_{e^+e^-}^{\text{1-loop}}$, pb	15.465(2)	15.870(2)	13.861(1)	17.884(2)
δ , %	7.56(1)	5.59(1)	9.09(1)	3.05(1)
$\sqrt{s} = 1000 \text{ GeV}$				
$\sigma_{e^+e^-}^{\text{Born}}$, pb	3.67921(1)	3.90568(1)	3.03577(3)	4.77562(5)
$\sigma_{e^+e^-}^{\text{1-loop}}$, pb	3.8637(4)	3.9445(4)	3.2332(3)	4.6542(7)
δ , %	5.02(1)	0.99(1)	6.50(1)	-2.54(1)

$e^+e^- \rightarrow e^+e^-$: distributions in $\cos\theta$

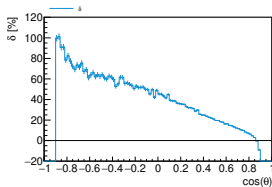
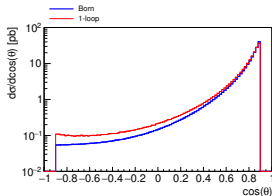
$\sqrt{s} = 250$ GeV



$\sqrt{s} = 500$ GeV



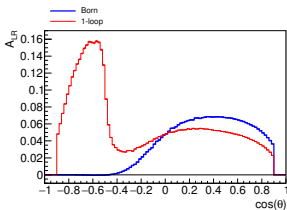
$\sqrt{s} = 1000$ GeV



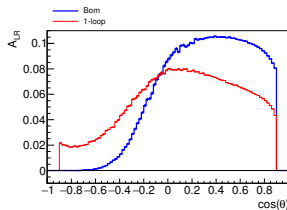
$e^+e^- \rightarrow e^+e^-$: A_{LR} distributions in $\cos\theta$

$$A_{LR} = \frac{\sigma_{LR} - \sigma_{RL}}{\sigma_{LR} + \sigma_{RL}}$$

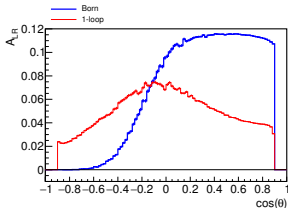
$\sqrt{s} = 250$ GeV



$\sqrt{s} = 500$ GeV



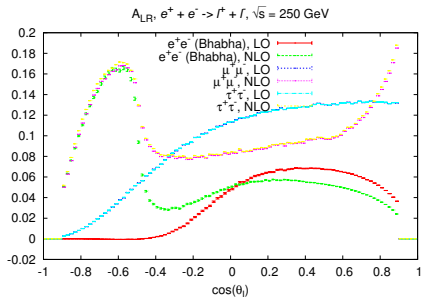
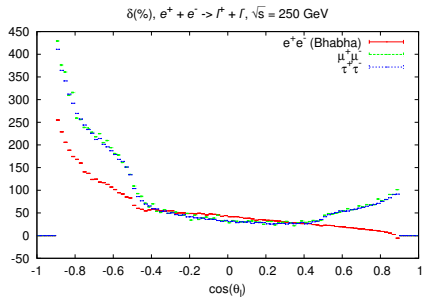
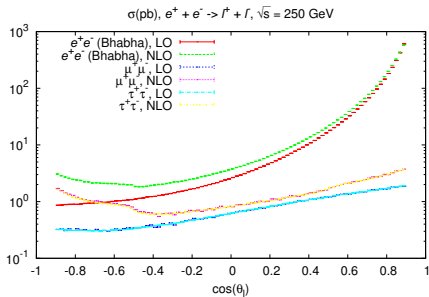
$\sqrt{s} = 1000$ GeV



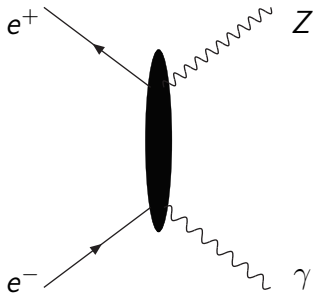
$e^+e^- \rightarrow \ell^+\ell^-$: Born vs 1-loop (preliminary)

P_{e^-}, P_{e^+}	0, 0	-0.8, 0	-0.8, -0.6	-0.8, 0.6
$\sqrt{s} = 250 \text{ GeV}$				
$e^- + e^+ \rightarrow e^- + e^+$ (Bhabha)				
$\sigma_{e^+e^-}^{\text{Born}}$, pb	56.6763(1)	57.7738(1)	56.2725(4)	59.2753(5)
$\sigma_{e^+e^-}^{\text{1-loop}}$, pb	61.731(6)	62.587(6)	61.878(6)	63.287(7)
δ , %	8.92(1)	8.33(1)	9.96(1)	6.77(1)
$e^- + e^+ \rightarrow \mu^- + \mu^+$				
$\sigma_{e^+e^-}^{\text{Born}}$, pb	1.4174(1)	1.5462(1)	0.7690(2)	2.3231(2)
$\sigma_{e^+e^-}^{\text{1-loop}}$, pb	2.3987(2)	2.616(2)	1.3015(1)	3.929(1)
δ , %	69.22(2)	69.13(1)	69.18(2)	69.12(1)
$e^- + e^+ \rightarrow \tau^- + \tau^+$				
$\sigma_{e^+e^-}^{\text{Born}}$, pb	1.4174(1)	1.5461(1)	0.7692(1)	2.3230(1)
$\sigma_{e^+e^-}^{\text{1-loop}}$, pb	2.3609(1)	2.5773(1)	1.2817(1)	3.8728(2)
δ , %	66.56(1)	66.69(1)	66.62(1)	66.71(1)

$e^+e^- \rightarrow l^+l^-$: distributions in $\cos\theta_l$ (preliminary)



$$e^+e^- \rightarrow Z\gamma$$



The expressions for HA and the results for unpolarized case were published in [Eur.Phys.J.C54:187-197,2008](#)

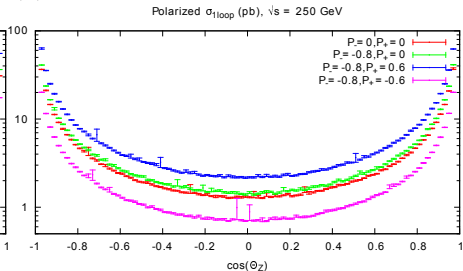
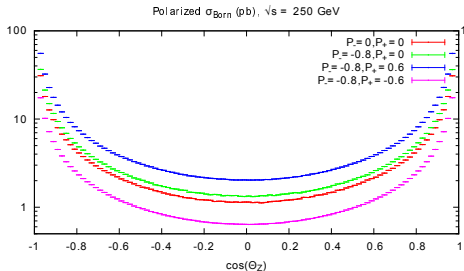
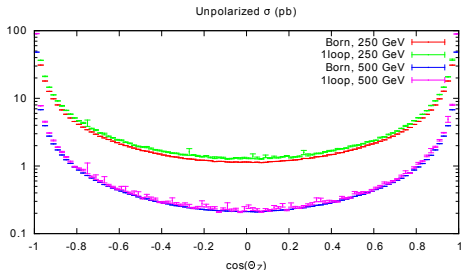
Here we present the preliminary results for 1-loop corrections taking into account the effect of polarization of e^+e^- beams.

$e^+e^- \rightarrow Z\gamma$: Born vs 1-loop (preliminary)

\sqrt{s}	250	500	1000
$\sigma_{Z\gamma}^{\text{Born}}$, pb	15.7038(6)	3.3858(3)	0.81958(3)
$\sigma_{Z\gamma}^{\text{1-loop}}$, pb	24.37(1)	5.23(6)	1.237(3)
δ , %	55.20(6)	54.4(2)	50.9(4)

P_{e^-}, P_{e^+}	0, 0	-0.8, 0	-0.8, 0.6	-0.8, -0.6
$\sqrt{s} = 250$ GeV				
$\sigma_{Z\gamma}^{\text{Born}}$, pb	15.7038(6)	18.520(4)	28.174(2)	8.870(3)
$\sigma_{Z\gamma}^{\text{1-loop}}$, pb	24.37(1)	28.00(1)	42.13(2)	13.53(1)
δ , %	55.20(6)	51.11(8)	49.55(7)	52.57(9)

$e^+e^- \rightarrow Z\gamma$: distributions in $\cos\theta_Z$ (preliminary)



Conclusions and plans

- We are building a powerful team of experimentalists and theoreticians that will prepare the physics research at the next generation e^+e^- collider
- We created the FORTRAN modules for polarized Bhabha scattering with complete one-loop EW corrections. Based on these modules Monte Carlo generator [Phys.Rev. D98 (2018) no.1, 013001] of unweighted events was created with possibility to produce events in Les Houches Event format
- Preliminary results for polarized $e^+e^- \rightarrow \mu^+\mu^-$, $e^+e^- \rightarrow \tau^+\tau^-$ (the paper in preparation) and $e^+e^- \rightarrow Z\gamma$ were presented. More processes will be included in MC generator in the future